

Supporting Information

Induced Amphotropic and Thermotropic Ionic Liquid Crystallinity in Phosphonium Halides. “Lubrication” by Hydroxyl Groups.

Kefeng Ma,^a B. S. Somashekhar,^b G. A. Nagana Gowda,^{b,c} C. L. Khetrapal,^b and Richard G. Weiss^{a*}

Department of Chemistry, Georgetown University, Washington, D.C. 20057-1227, USA and Center of Biomedical Magnetic Resonance, Sanjay Gandhi Post Graduate Institute of Medical Sciences, Lucknow-226 014, India

Email: weissr@georgetown.edu

Syntheses

***tri*-Decyl-(2-hydroxyethyl)phosphonium bromide (2P10OHBr).** In a glove box purged with nitrogen, *tri*-decylphosphine (13.98 g, 30.8 mmol) was transferred into a round-bottom flask containing a stirring bar. Nitrogen was bubbled through a mixture of 120 mL chloroform and 2-bromoethanol (4.62 g, 37.0 mmol) in another sealed flask for ca. 15 min before being added by syringe to the flask with the phosphine. The solution was stirred for one day at room temperature under nitrogen. Removal of volatile liquids on a rotary evaporator left a clear oil, which was subsequently crystallized thrice from ethyl ether at -77 °C and filtered on a Büchner funnel packed in dry-ice to afford 12.5g (70%) of a deformable, hygroscopic solid.

***tri*-Decyl-(2-hydroxyethyl)phosphonium chloride (2P10OHCl).** A mixture of 0.50 g (0.86 mmol) **2P10OHBr** and 0.17 g (1.06 mmol) potassium ethyl xanthate in 50 mL chloroform was stirred in a round-bottom flask at room temperature for one day

^a Department of Chemistry, Georgetown University, Washington, D.C. 20057-1227, USA.

^b Center of Biomedical Magnetic Resonance, Sanjay Gandhi Post Graduate Institute of Medical Sciences, Lucknow 226 014, India.

^c Current address: Department of Chemistry, Purdue University, West Lafayette, IN 47907, USA.

and then gravity filtered. Conc. hydrochloric acid (0.1 mL, 1.22 mmol) was subsequently added while the solution was cooled in an ice bath. After being stirred for one day, the organic layer was washed with water (3×25 mL) and reduced to a colorless oil on a rotary evaporator. The oil was crystallized three times from ethyl acetate at -77 °C and filtered on a Büchner funnel packed in dry-ice to provide 0.28 g (61%) of a deformable, hygroscopic solid.

1PnBr and **1PnCl** (n = 10, 14, 18) were synthesized according to reported procedures.¹

tri-Decylmethylphosphonium chloride (1P10Cl). T_{K-I} : 103.2 – 105.2 (lit. 96.2 - 97.9 °C^{1a}). ¹H NMR (CDCl₃): δ 2.45 (m, 6H), 2.13 (d, 3H, ² J_{PCH_3} = 13.5 Hz), 1.51 (m, 12H), 1.26 (m, 36H), 0.88 (t, 9H) ppm. ¹³C NMR (CDCl₃): δ 32.35, 31.22 (d, ³ J_{PCCC} = 15.0 Hz), 29.97, 29.82, 29.76, 29.54, 23.15, 22.30 (d, ² J_{PCC} = 4.5 Hz), 20.89 (d, ¹ J_{PCH_2} = 48.8 Hz), 14.60, 5.52 (d, ¹ J_{PCH_3} = 52.4 Hz) ppm. ³¹P NMR (CDCl₃): δ 32.2 ppm. Anal. Calcd. for C₃₁H₆₆ClP: C, 73.69; H, 13.17. Found: C, 73.27; H, 13.61. (Note: No weight loss was observed by TGA when this sample was heated to 100 °C.

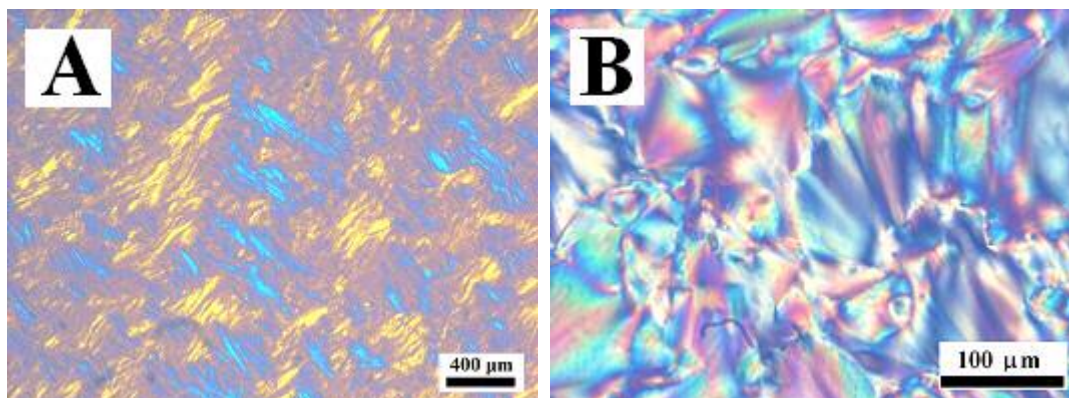
Methyl-tri-tetradecylphosphonium chloride (1P14Cl). T_{K-I} : 106.2–107.1 °C (lit. 105.0–105.5 °C^{1b}). ¹H NMR (CDCl₃): δ 2.46 (m, 6H), 2.14 (d, 3H, ² J_{PCH_3} = 13.5 Hz), 1.50 (m, 12H), 1.26 (m, 60H), 0.88 (t, 9H) ppm. ¹³C NMR (CDCl₃): δ 32.53, 31.31 (d, ³ J_{PCCC} = 15.1 Hz), 30.26 (broad singlet from overlapping peaks), 30.13, 29.96, 29.92, 29.66, 23.30, 22.30 (d, ² J_{PCC} = 4.5 Hz), 20.97 (d, ¹ J_{PCH_2} = 48.3 Hz), 14.73, 5.64 (d, ¹ J_{PCH_3} = 51.8 Hz) ppm. ³¹P NMR (CDCl₃): δ 32.64 ppm.

Methyl-tri-octadecylphosphonium chloride (1P18Cl). T_{K-I} : 100.8–101.6 (lit. 95.5-97.5 °C^{1b}). ¹H NMR (CDCl₃): δ 2.45 (m, 6H), 2.13 (d, 3H, ² J_{PCH_3} = 3.5 Hz), 1.50 (m, 12H), 1.25 (m, 84H), 0.88 (t, 9H) ppm. ¹³C NMR (CDCl₃): δ 32.59, 31.34 (d, ³ J_{PCCC} = 15.0 Hz), 30.32 (broad singlet from overlapping peaks), 30.17, 30.02, 29.97, 29.70, 23.35, 22.44 (d, ² J_{PCC} = 4.5 Hz), 21.00 (d, ¹ J_{PCH_2} = 49.3 Hz), 14.78, 5.68 (d, ¹ J_{PCH_3} = 51.8 Hz) ppm. ³¹P NMR (CDCl₃): δ 32.67 ppm.

tri-Decylmethylphosphonium bromide (1P10Br). T_{K-I} : 98.8–100.7 °C (lit. 97.5–99.5 °C^{1a}). ^1H NMR (CDCl_3): δ 2.45 (m, 6H), 2.13 (d, 3H, $^2J_{\text{POCH}_3} = 13.5$ Hz), 1.50 (m, 12H), 1.26 (m, 36H), 0.88 (t, 9H) ppm. ^{13}C NMR (CDCl_3): δ 32.37, 31.23 (d, $^3J_{\text{PCCC}} = 15.0$ Hz), 30.00, 29.85, 29.78, 29.56, 23.18, 22.32 (d, $^2J_{\text{PCC}} = 4.5$ Hz), 21.08 (d, $^1J_{\text{POCH}_2} = 48.9$ Hz), 14.62, 5.81 (d, $^1J_{\text{POCH}_3} = 52.4$ Hz) ppm. ^{31}P NMR (CDCl_3): δ 32.33 ppm. . Anal. Calcd. for $\text{C}_{31}\text{H}_{66}\text{BrP}$: C, 67.73; H, 12.10. Found: C, 67.48; H: 12.40.

Methyl-tri-tetradecylphosphonium bromide (1P14Br). $T_{K-\text{SmA}2}$: 103.6– 104.7 °C (lit. 103.5 °C^{1b}); $T_{\text{SmA}2-I}$: 113.2–114.0 °C (lit. 112.4 °C^{1b}). ^1H NMR (CDCl_3): δ 2.47 (m, 6H), 2.14 (d, 3H, $^2J_{\text{POCH}_3} = 13.8$ Hz), 1.50 (m, 12H), 1.26 (m, 60H), 0.88 (t, 9H) ppm. ^{13}C NMR (CDCl_3): δ 32.44, 31.22 (d, $^3J_{\text{PCCC}} = 14.6$ Hz), 30.17 (broad singlet from overlapping peaks), 30.06, 29.88, 29.57, 23.20, 22.32 (d, $^2J_{\text{PCC}} = 4.5$ Hz), 21.07 (d, $^1J_{\text{POCH}_2} = 48.3$ Hz), 14.63, 5.94 (d, $^1J_{\text{POCH}_3} = 52.4$ Hz) ppm. ^{31}P NMR (CDCl_3): δ 32.25 ppm.

Methyl-tri-octadecylphosphonium bromide (1P18Br). $T_{K-\text{SmA}2}$: 95.9–97.1 °C (lit. 99.4 °C^{1b}); $T_{\text{SmA}2-I}$: 106.2–107.2 °C (lit. 106.9 °C^{1b}). ^1H NMR (CDCl_3): δ 2.46 (m, 6H), 2.14 (d, 3H, $^2J_{\text{POCH}_3} = 13.5$ Hz), 1.51 (m, 12H), 1.26 (m, 84H), 0.88 (t, 9H) ppm. ^{13}C NMR (CDCl_3): δ 32.55, 31.32 (d, $^3J_{\text{PCCC}} = 14.5$ Hz), 30.34 (broad singlet from overlapping peaks), 30.17, 29.99, 29.68, 23.32, 22.42 (d, $^2J_{\text{PCC}} = 4.5$ Hz), 21.16 (d, $^1J_{\text{POCH}_2} = 47.8$ Hz), 14.75, 5.96 (d, $^1J_{\text{POCH}_3} = 52.4$ Hz) ppm. ^{31}P NMR (CDCl_3): δ 32.31 ppm.



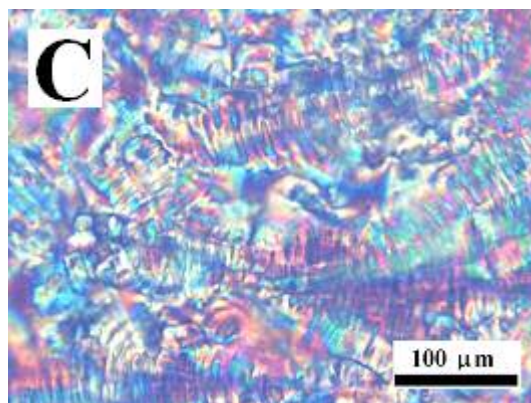
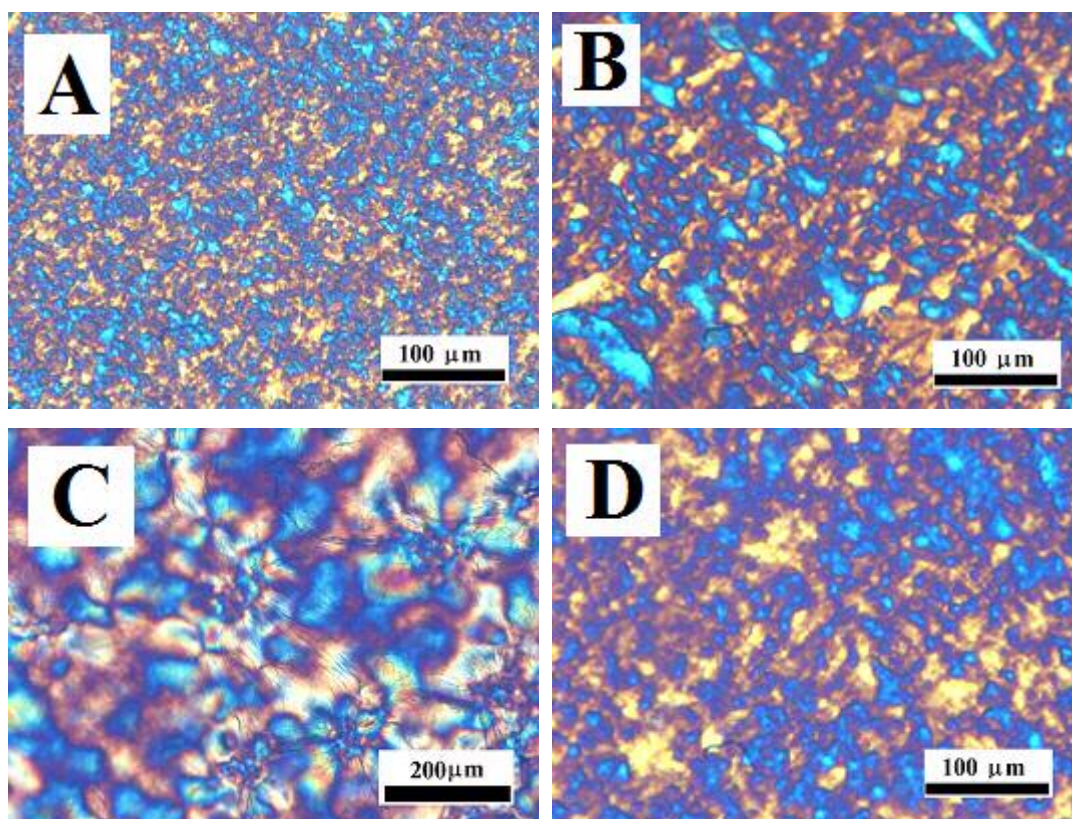


Figure S1. Polarized optical micrographs (POMs) of liquid-crystalline samples after applying lateral force on their cover slips: (A) **1P10Br•CH₃OH** (5.5 wt % (1.0 equivalent) methanol) at 8 °C, streak texture; (B) **1P14Br•CH₃OH** (4.3 wt % (1.0 equivalent) methanol) at 65.6 °C, fan-shaped texture; and (C) **1P14Cl•CH₃OH** (4.5 wt % (1.0 equivalent) methanol) at 68.5 °C, banded fan-shaped texture.



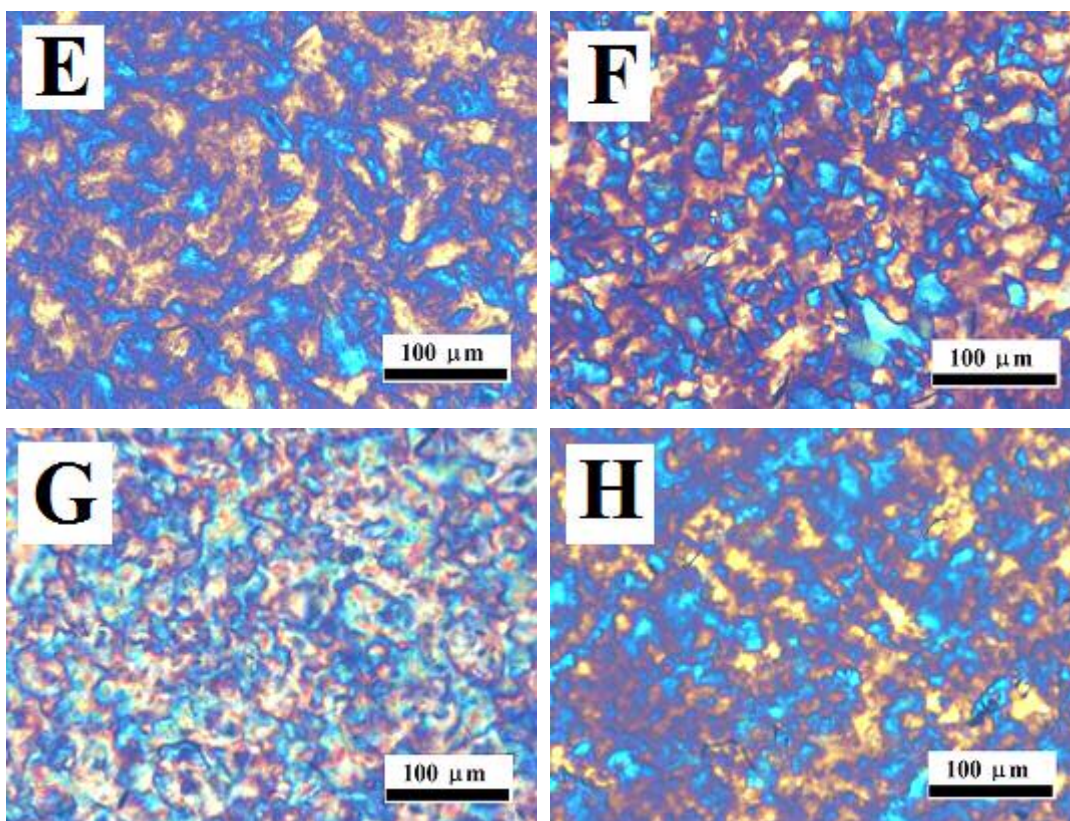


Figure S2. Polarized optical micrographs of **1PnX** and **1PnX•CH₃OH** (n=14, 18) after being cooled to room temperature (24 °C) from their isotropic phases: (A) **1P14Cl•CH₃OH** (4.5 wt % (1.0 equivalent) methanol), (B) **1P14Cl**, (C) **1P14Br•CH₃OH** (4.3 wt % (1.0 equivalent) methanol), (D) **1P14Br**, (E) **1P18Cl•CH₃OH** (3.7 wt % (1.0 equivalent) methanol), (F) **1P18Cl**, (G) **1P18Br•CH₃OH** (3.5 wt % (1.0 equivalent) methanol), (H) **1P18Br**.

Table S1. Weight loss from **1PnX•CH₃OH** over specific temperature ranges.

Samples (wt% CH ₃ OH ^a)	Temperature Range (°C)	Weight Loss (%) ^c
1P10Cl•CH₃OH (6.00)	96- 114	5.56
1P14Cl•CH₃OH (4.54)	41 - 70	2.48
1P18Cl•CH₃OH (3.67)	25 - 100	1.13
	100 - 200	0.07
1P10Br•CH₃OH (5.50)	94 - 116	5.07
1P14Br•CH₃OH (4.27)	61 - 89	3.18
1P18Br•CH₃OH (3.49)	25 - 100	1.39

	100 - 200	0.22
1P18Br·CH₃OH (3.49) ^b	38 - 63	2.45

^a The weight percents of the added methanol in the **1PnX·CH₃OH** are shown in parentheses.

^b Cooled rapidly after 10 h at 100 °C to room temperature in the air.

Table S2. Lamellar spacings (d) from X-ray diffraction data for liquid-crystalline **1P14Br**, **1P18Br**, **2P14OHBr** and **1P14Br•CH₃OH**.

1P14Br		1P18Br		2P14OHBr		1P14Br•CH₃OH		2P10OHBr	
T (°C)	d (Å)	T (°C)	d (Å)	T (°C)	d (Å)	T (°C)	d (Å)	T (°C)	d (Å)
24	28.1	24	35.0	24.	25.6	24	27.7	24	22.0
49.5	28.1	44	35.2	37.5	25.6	34.5	27.6	39.5	22.0
60	28.3	68.5	35.3	51	25.6	38	27.6	47	22.0
65	29.6	83	35.5	54	25.3	43	27.2	48	20.9
69	29.9	85	37.7	58	25.6	46	27.0	49.5	20.6
78.5	29.9	86	38.3	60.5	26.6	49	26.8	50.5	20.5
86.5	29.7	92.5	38.6	62	27.3	51	27.1	52.5	20.4
96.5	29.6	95.5	39.1	71	26.8	53.5	27.3	57	20.3
101	29.5	99	39.1	79.5	26.5	55	27.4	63.5	20.3
103.5	29.4	99.5	35.4	91	25.9	58	27.2	66.5	20.3
104.5	27.1	100	31.9	97	25.8	66	26.5	67	20.0
106	26.6	103	31.1	98	25.6	74.5	25.8	67.5	19.9
109	26.3	106	30.7	99	25.1	77	25.5	68.5	19.7
112	26.2	106.5	29.1	106	24.6	79	24.5	73.5	19.6
114	25.6	107	28.5	116.5	24.3	83	24.1	77.5	19.6
115	25.4	109.5	28.2	130	24.0	94	24.0		
116.5	25.1	113	27.9						
122	24.7	124	27.6						

Table S3. Lamellar spacings (d) from X-ray diffraction data for liquid-crystalline **2PnOHCl** and **1P14Cl•CH₃OH**.

2P10OHCl		2P14OHCl		1P14Cl•CH₃OH			2P18OHCl	
T (°C)	d (Å)	T (°C)	d (Å)	T (°C)	d_1 (Å)	d_2 (Å)	T (°C)	d (Å)
24	22.7	24	26.5	24		28.3	24	32.8
38	22.6	40	26.4	38		28.2	43.5	32.8
44.5	22.6	48	26.3	46		28.2	56.5	32.7
45.5	21.1	57	26.2	55		28.1	69.5	32.7
47	21.1	60	26.3	57		28.1	77	32.7
51	21.0	65.5	26.4	59		28.2	84	32.6
59.5	20.8	67.5	27.0	59.5	26.4	31.5	86	32.3
67	20.7	68	27.8	61	26.4	31.4	87	31.5
74	20.6	71	27.7	62	26.2	30.9	88	31.4
76	20.5	76.5	27.5	64	26.2	30.6	90.5	31.0
78	20.2	82	27.1	64.5	26.2	30.4	93.5	30.5
83.5	20.2	85.5	26.6	65	26.9		94	29.0
94.5	20.1	89.5	26.4	67.5	26.6		95	28.8
		93.5	26.1	70.5	26.4		100	28.6
		97.5	25.8	75.5	25.9		109	28.2
		98	25.6	77	24.6		117	27.8
		99	24.6	78.5	24.3		127	27.5
		103.5	24.5	81.5	24.1			
		109.5	24.4	86	24.1			
		111	24.2					

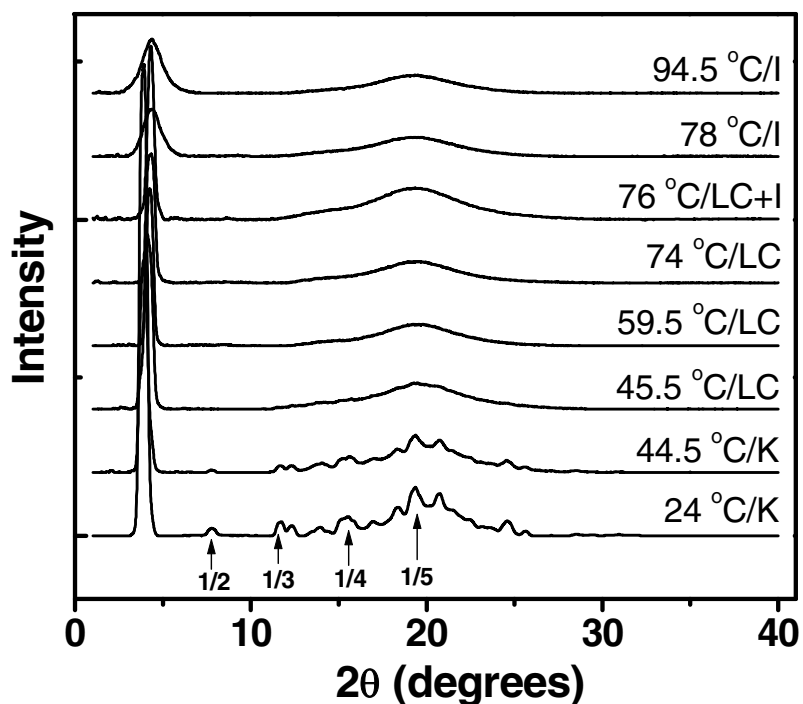


Figure S3. X-ray diffraction stack plots of diffractograms of **2P10OHCl** at various temperatures and in different phases. The spacing ratios (marked by arrows) assuming a lamellar structure are indicated. Only some of the diffractograms recorded are included here for clarity.

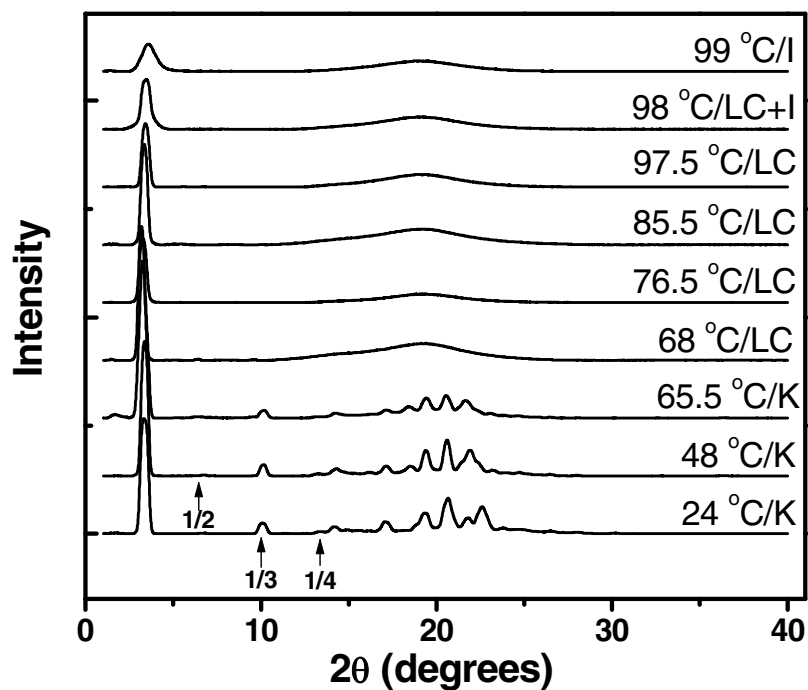


Figure S4. X-ray diffraction stack plots of diffractograms of **2P14OHCl** at various temperatures and in different phases. The spacing ratios (marked by arrows) assuming a lamellar structure are indicated. Only some of the diffractograms recorded are included here for clarity.

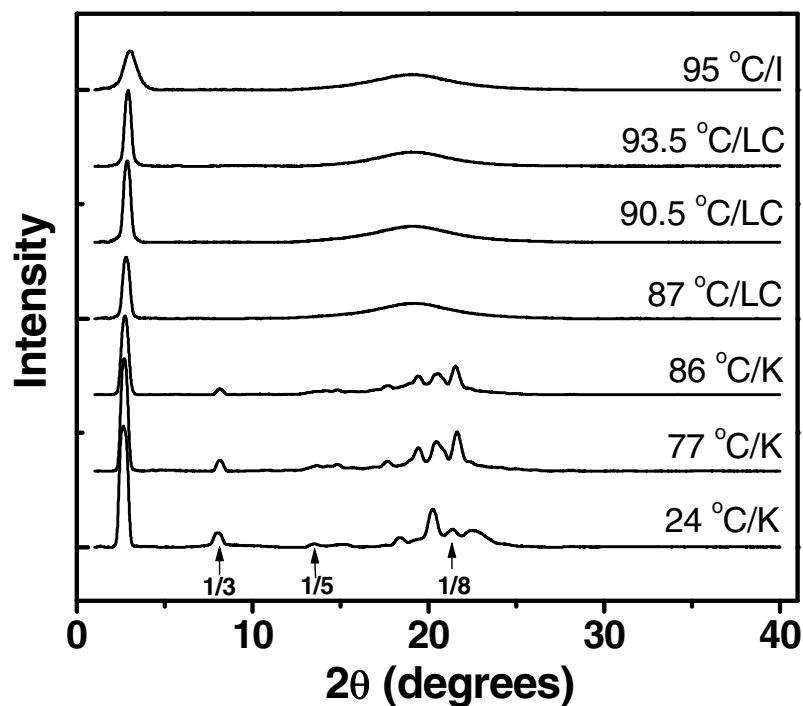


Figure S5. X-ray diffraction stack plots of diffractograms of **2P18OHCl** at various temperatures and in different phases. The spacing ratios (marked by arrows) assuming a lamellar structure are indicated. Only some of the diffractograms recorded are included here for clarity.

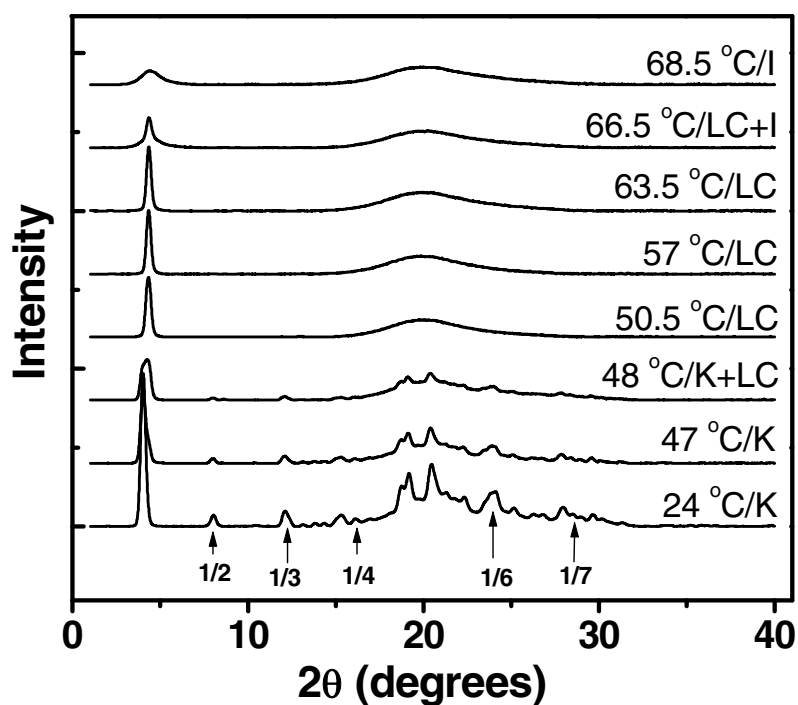


Figure S6. X-ray diffraction stack plots of diffractograms of **2P10OHBr** at various temperatures and in different phases. The spacing ratios (marked by arrows) assuming a lamellar structure are indicated. Only some of the diffractograms recorded are included here for clarity.

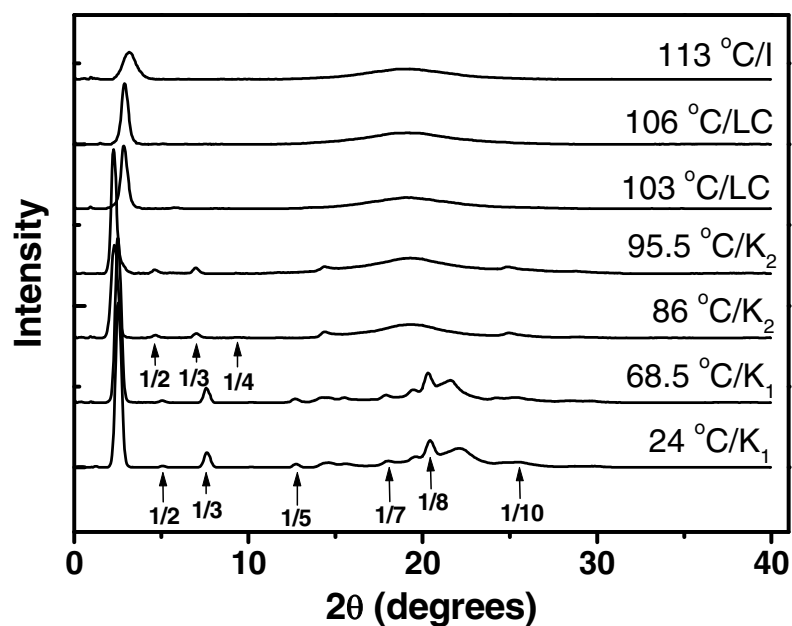


Figure S7. X-ray diffraction stack plots of diffractograms of **1P18Br** at various temperatures and in different phases. The spacing ratios (marked by arrows) assuming a lamellar structure are indicated. Only some of the diffractograms recorded are included here for clarity. The $1/4$ peak at 86 °C is discernible when the diffractogram is intensified.

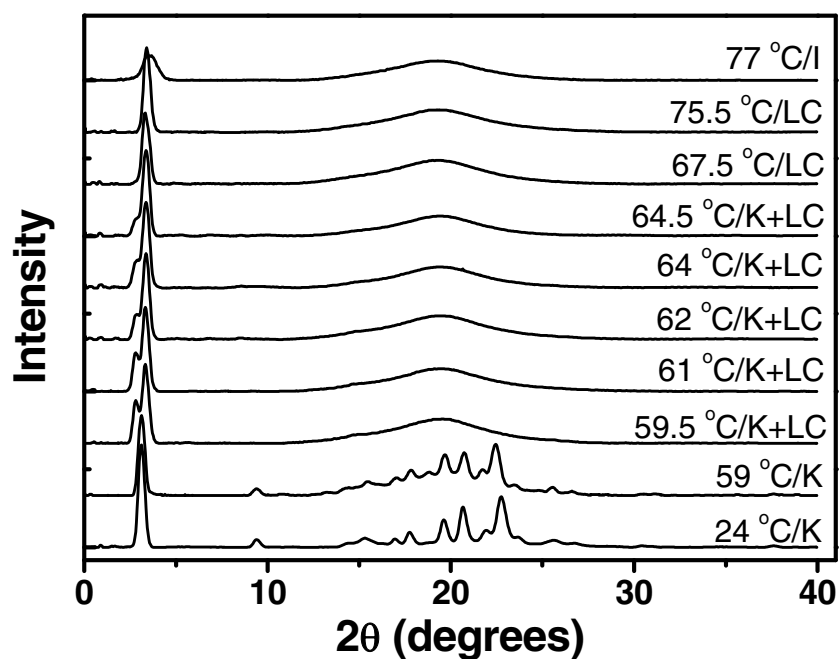


Figure S8. X-ray diffraction stack plots of diffractograms of **1P14Cl•CH₃OH** (4.5 wt% (1.0 equivalent) CH₃OH) at various temperatures and in different phases. Only some of the diffractograms recorded are included here for clarity.

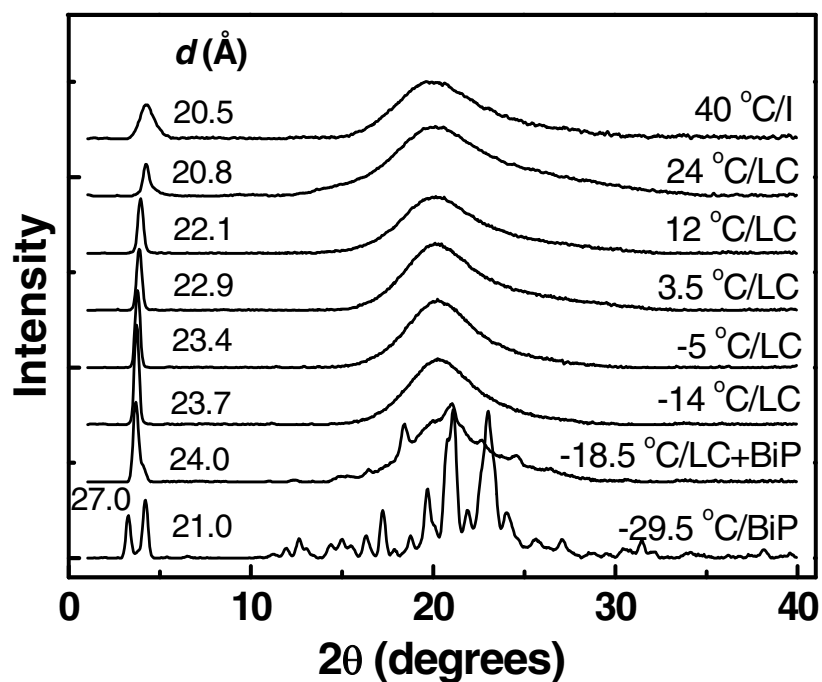


Figure S9. X-ray diffraction stack plots of diffractograms of **1P10Cl•CH₃OH** (6.0 wt% (1.0 equivalent) CH₃OH) at various temperatures and in different phases.

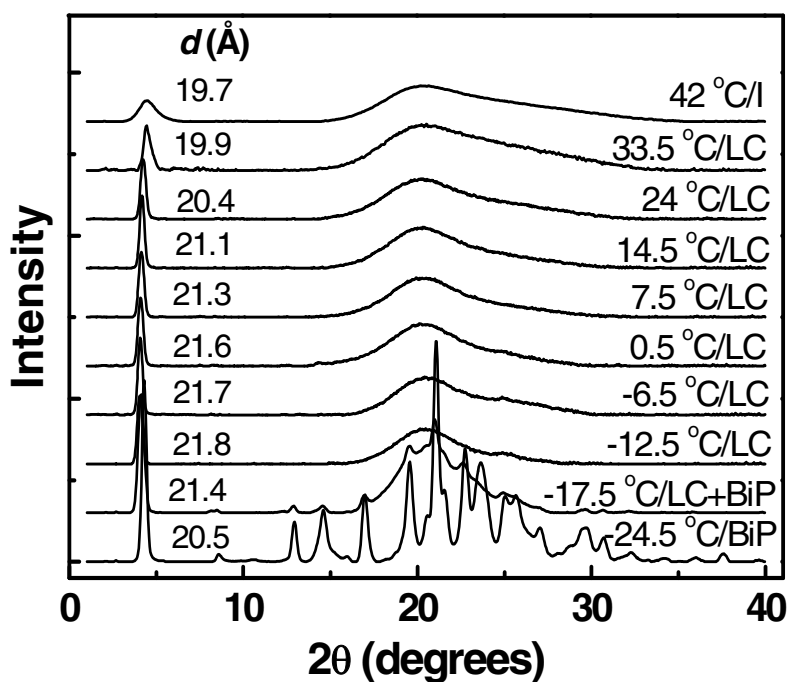


Figure S10. X-ray diffraction stack plots of diffractograms of **1P10Br•CH₃OH** (5.5 wt% (1.0 equivalent) CH₃OH) at various temperatures and in different phases.

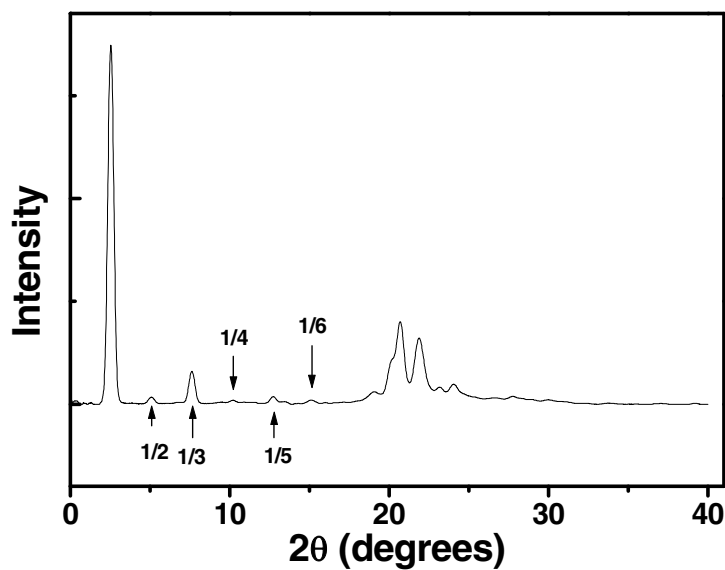


Figure S11. X-ray diffractogram of **2P18OHBr** in its solid phase at 24 °C. The spacing ratios assuming a lamellar structure are marked by arrows.

Table S4. Lamellar spacings (d) from X-ray diffraction data for nonmesogenic **1PnCl** and **1P10Br**.

1P10Cl		1P14Cl		1P18Cl		1P10Br	
T (°C)	d (Å)	T (°C)	d (Å)	T (°C)	d (Å)	T (°C)	d (Å)
-35.5	21.1	24	28.3	24	35.5	-35.5	21.0
-22.5	21.2	39	28.4	49	35.7	-22.5	21.1
-14.5	21.3	57	28.6	70	35.9	-9.5	21.1
-4.5	21.3	65	28.9	85.5	36.1	5.5	21.1
5	21.4	67	29.7	89	36.3	10	21.7
9.5	22.3	69.5	31.2	91	36.4	13.5	22.0
14	23.2	70.5	31.8	92	37.6	14.5	22.0
15.5	23.3	79	31.8	93	38.7	20	22.1
24	23.4	83.5	31.8	95	39.8	24	22.1
38	23.3	90	31.7	100.5	39.8	38	22.1
54.5	23.3	104	31.4	102	39.7	53.5	22.1
71.5	23.2	107	31.4	103	28.4	69	22.1
91	23.2	108	31.2	110	28.0	87	22.1
103	23.1	109.5	24.6			97.5	22.1
105.5	21.0	116	24.3			98.5	21.9
107	20.0					100.5	20.7
113.5	19.9					102.5	19.8
						114	19.6

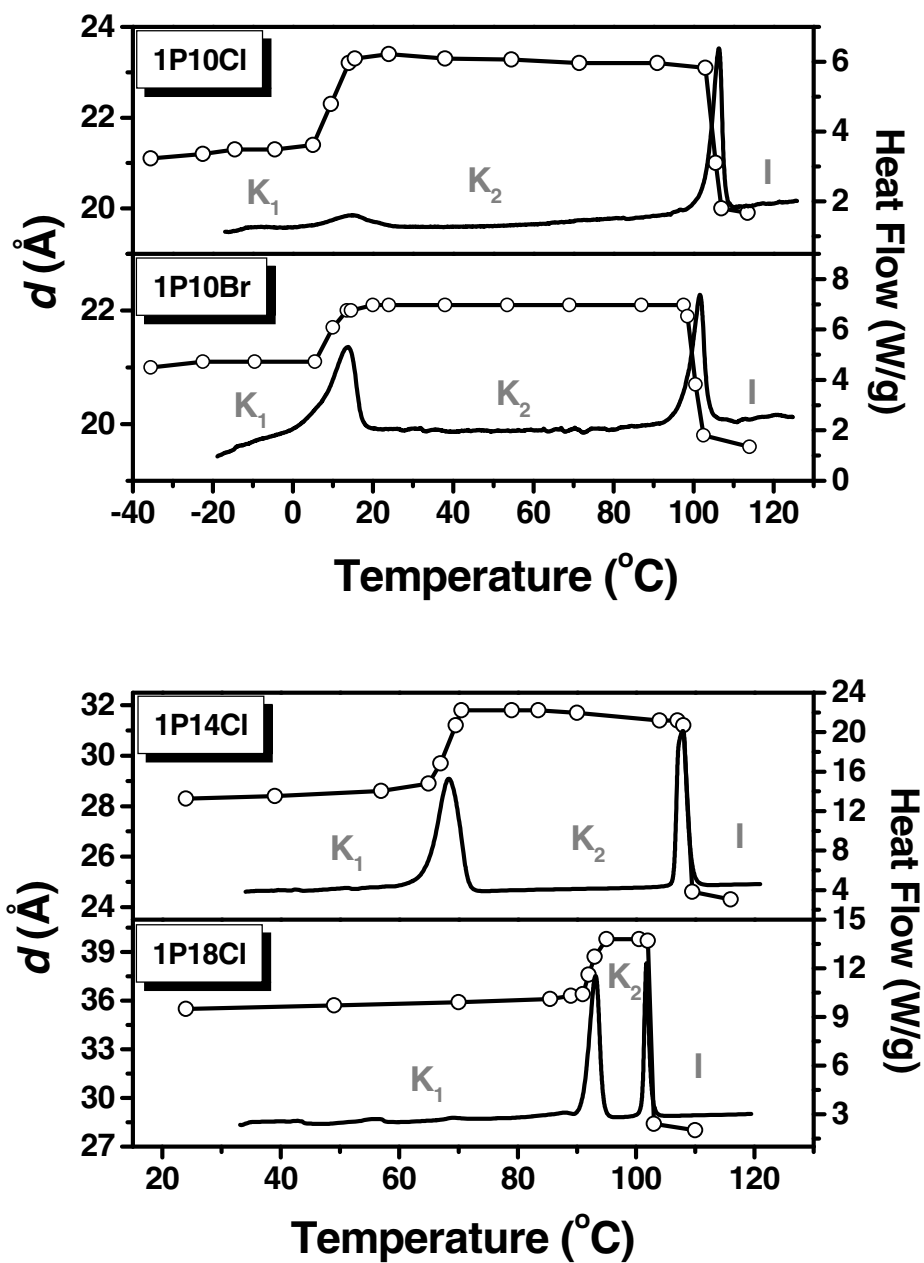


Figure S12. Heat flow from DSC thermograms (2nd heating; 5 °C/min) (full lines) and lamellar spacings (d) from X-ray diffraction (o) at different temperatures for some nonmesogenic **1PnCl** and **1PnBr**.

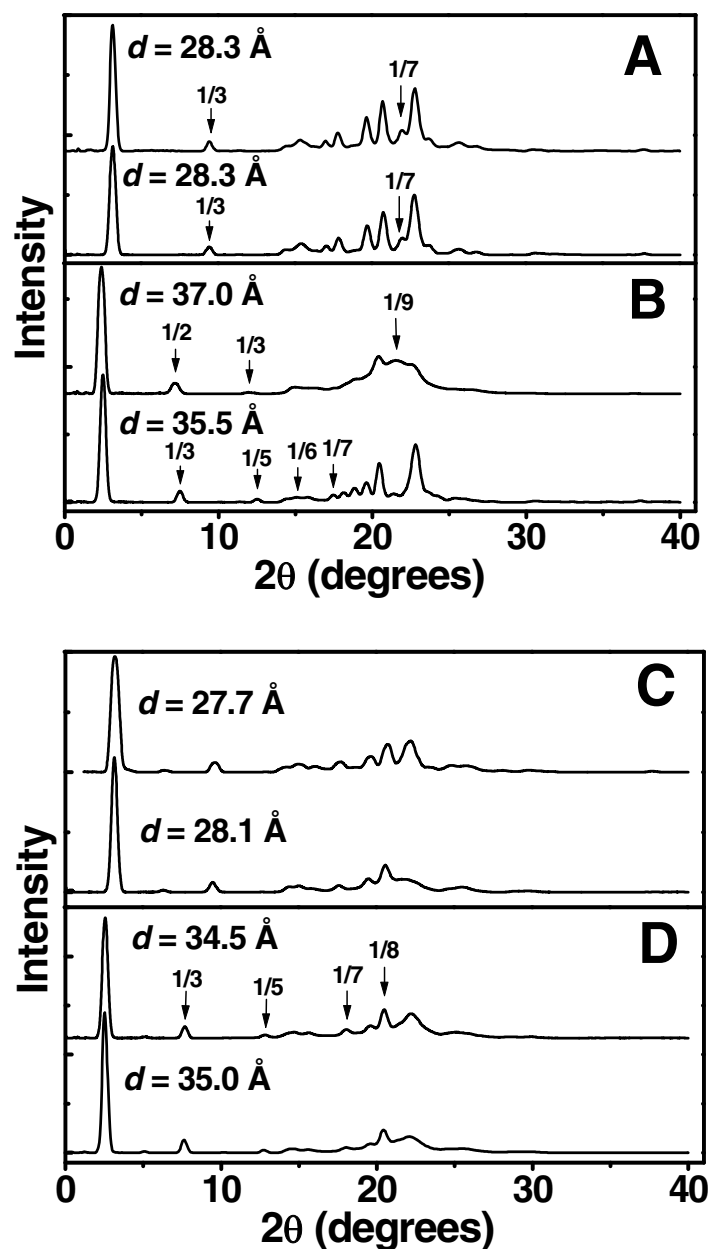


Figure S13. X-ray diffractograms of **1PnX** (lower in each box) and **1PnX·CH₃OH** (upper in each box) at 24 °C in their solid phases (prepared by cooling from their isotropic phases): (A) **1P14Cl** and **1P14Cl·CH₃OH** (4.5 wt % (1.0 equivalent) methanol), (B) **1P18Cl** and **1P18Cl·CH₃OH** (3.7 wt % (1.0 equivalent) methanol), (C) **1P14Br** and **1P14Br·CH₃OH** (4.3 wt % (1.0 equivalent) methanol), and (D) **1P18Br** and **1P18Br·CH₃OH** (3.5 wt % (1.0 equivalent) methanol). The spacing ratios, assuming lamellar structures, are indicated by arrows.

Table S5. The rates of change of lamellar spacings with temperature ($\Delta d/\Delta T$) in K and SmA₂ phases. In some cases, the changes of $\Delta d/\Delta T$ are not very linear in K phases, but the absolute changes in d are very small.

Phosphonium salts (n=10)	Phase	$\Delta d/\Delta T$ (Å/°C)	R	Phosphonium salts (n=14)	Phase	$\Delta d/\Delta T$ (Å/°C)	R	Phosphonium salts (n=18)	Phase	$\Delta d/\Delta T$ (Å/°C)	R
1P10Cl	K ₁	0.0039	0.97	1P14Cl	K ₁	0.014	0.92	1P18Cl	K ₁	0.013	0.97
	K ₂	-0.0027	0.92		K ₂	-0.011	-0.92		K ₂	-0.015	-0.67
2P10OHCl	K	-0.0061	-0.99	2P14OHCl	K	-0.0065	-0.96	2P18OHCl	K	-0.0028	-0.88
	SmA ₂	-0.019	-0.99		SmA ₂	-0.074	-0.99		SmA ₂	-0.15	-0.99
1P10Cl·CH₃OH	SmA ₂	-0.077	-0.98	1P14Cl·CH₃OH	K	-0.0026	-0.56	1P18Br	K ₁	0.0064	0.97
1P10Br	K ₁	0.0020	0.81		SmA ₂	-0.090	-1.00		K ₂	0.060	0.95
	K ₂	0.0008	0.55	1P14Br	K ₁	0.0034	0.73		SmA ₂	-0.20	-0.99
2P10OHBr	K	-0.0011	-0.75		K ₂	-0.014	-0.96				
	SmA ₂	-0.013	-0.87		SmA ₂	-0.075	-0.97				
1P10Br·CH₃OH	SmA ₂	-0.038	-0.95	2P14OHBr	K	-0.0030	-0.87				
					SmA ₂	-0.044	-1.00				
				1P14Br·CH₃OH	K	-0.037	-0.92				
					SmA ₂	-0.085	-1.00				

Infrared and Raman Spectroscopy (IR). The peak indicated by arrows at 580 cm^{-1} in the IR spectra of **1P10Br** containing one and two molar equivalents of methanol (Figure S14) is ascribed tentatively to the torsional motion of the OH group of methanol;² this band is found at 650 cm^{-1} in the neat liquid.³ We suggest that interactions between the hydroxyl proton and the bromide anion (rather than intermolecular methanol-methanol H-bonding, as in the neat liquid) causes the shift to lower energies. However, no analogous peaks were discernible in spectra of the corresponding chlorides (Figure S15).

A peak associated with hydrogen bonding between methanol and *tetra-*n*-heptylammonium* iodide shows a frequency at 255 cm^{-1} .⁴ Attempts to locate the interactions between the anions of our salts and the hydrogen of the hydroxyl group from the methanol solute or from the head group of the salts by Raman spectroscopy (Figures S16 and S17) were unsuccessful. No significant difference could be found in the $100\text{--}300\text{ cm}^{-1}$ when spectra of **2P10OHX**, **1P10X·CH₃OH** and **1P10X** were compared.

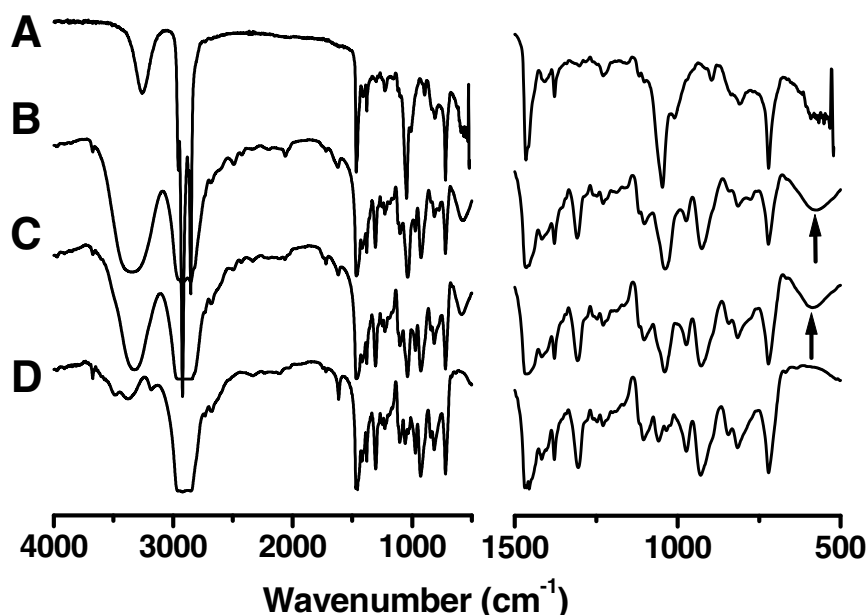


Figure S14. IR spectra of (A) **2P10OHBr**, (B) **1P10Br·2CH₃OH** (10.4 wt% (2.0 equivalents) methanol), (C) **1P10Br·CH₃OH** (5.5 wt% (1.0 equivalent) methanol), and (D) **1P10Br** at 24 °C. The CH₃OH torsional peaks in (B) and (C) are marked with an arrow.

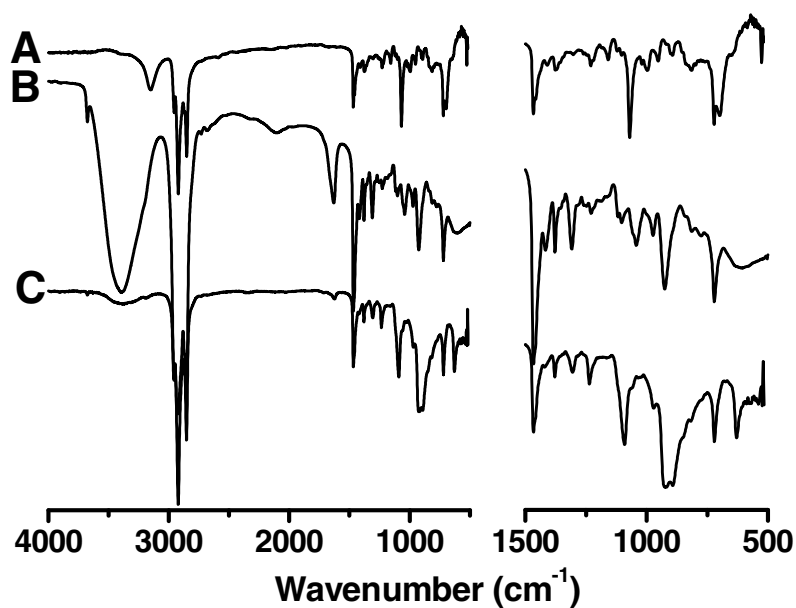


Figure S15. IR spectra of (A) 2P10OHCl, (B) 1P10Cl•CH₃OH (6.0 wt% (1.0 equivalent) methanol), and (C) 1P10Cl at 24 °C.

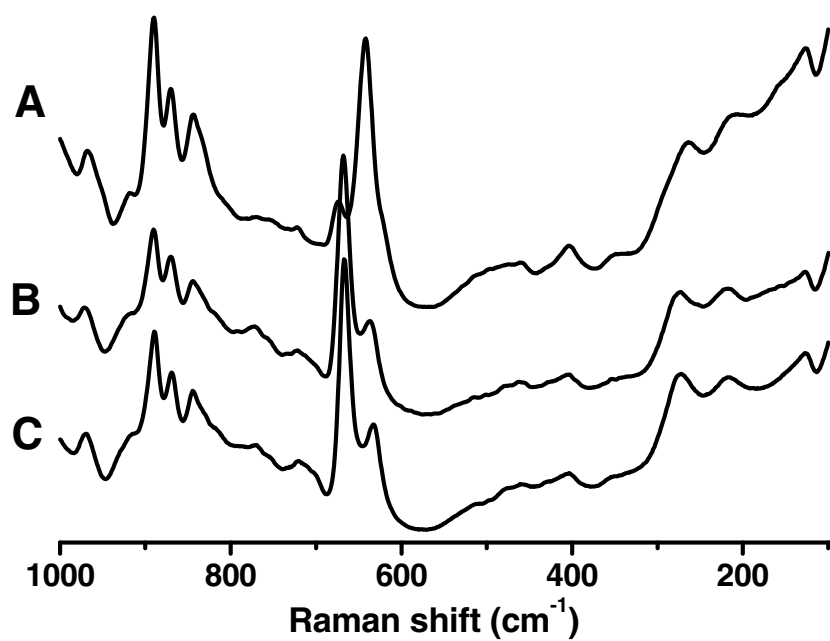


Figure S16. Raman spectra of (A) 2P10OHBr, (B) 1P10Br•CH₃OH (5.5 wt% (1.0 equivalent) methanol), and (D) 1P10Br at 24 °C.

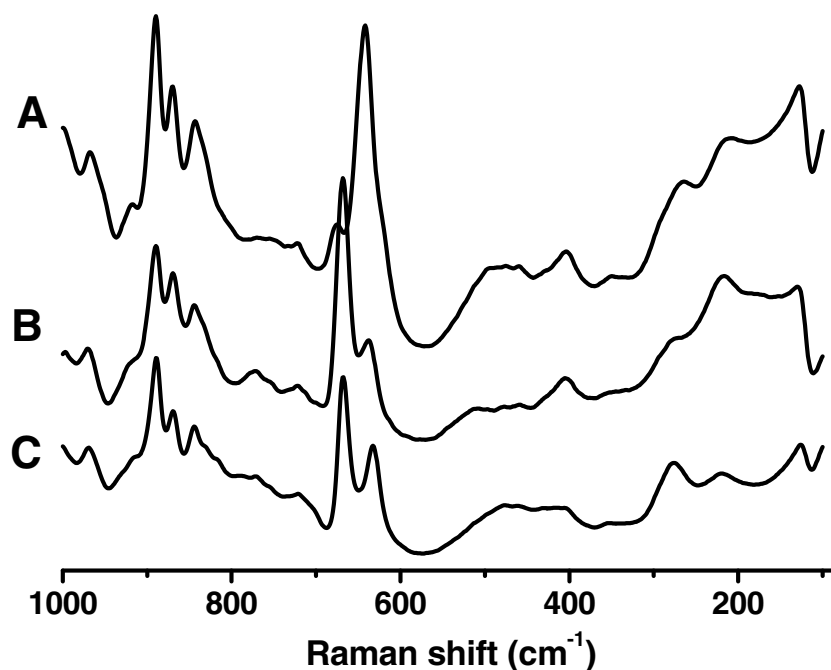


Figure S17. Raman spectra of (A) **2P10OHBr**, (B) **1P10Br•CH₃OH** (5.5 wt% (1.0 equivalent) methanol), and (D) **1P10Br** at 24 °C.

-
- (1) (a) Chen, H.; Kwait, D. C.; Gönen, Z. S.; Weslowski, B. T.; Abdallah, D. J.; Weiss, R. G. *Chem. Mater.* **2002**, *14*, 4063. (b) Abdallah, D. J.; Robertson, A.; Hsu, H.; Weiss, R. G. *J. Am. Chem. Soc.* **2000**, *122*, 3053.
- (2) Iwaki, L. K.; Dlott, D. D. *J. Phys. Chem. A* **2000**, *104*, 9101.
- (3) Schrader, B. *Raman/Infrared Atlas of Organic Compounds*, 2nd ed.; VCH: Weinheim, 1989, p A 3-03.
- (4) Singh, S.; Rao, N. R. *Trans. Faraday Soc.* **1966**, *62*, 3310.